

Article

Hydrochloric Acid Modification and Lead Removal Studies on Naturally Occurring Zeolites from Nevada, New Mexico, and Arizona.

Garven M. Huntley,^a Rudy L. Luck,^{a*} Michael E. Mullins,^b and Nick K. Newberry^a

^aDepartment of Chemistry and ^bDepartment of Chemical Engineering, Michigan Technological University, 1400 Townsend Drive, Houghton, MI 49931, USA.
E-mail: rluck@mtu.edu, 906 487 7137 (W), 906 487 2061 (F).

Abstract: Four naturally occurring zeolites AZLB-Ca and AZLB-Na (Bowie, Arizona), NM-Ca (Winston, New Mexico), and NV-Na (Ash Meadows, Nevada) were studied to evaluate structural modifications after treatment with HCl acid. AZLB-Ca and AZLB-Na are chabazite-like species and become amorphous when boiled in concentrated HCl acid as confirmed by powder X-ray diffraction. In contrast, NM-Ca and NV-Na which are clinoptilolite-like species withstood boiling in concentrated HCl acid. This treatment removes calcium, magnesium, sodium, potassium, aluminum, and iron atoms or ions from the framework while leaving the silicon framework intact as confirmed via X-ray fluorescence and diffraction. SEM images on calcined and HCl treated NV-Na were obtained. BET surface area analysis confirmed an increase in surface area for the two zeolites after treatment, NM-Ca (20.0(1) to 111(4) m²/g) and NV-Na (19.0(4) to 158(7) m²/g). ²⁹Si and ²⁷Al MAS NMR were performed on the natural and treated NV-Na zeolite and the data for the natural NV-Na zeolite suggested a Si:Al ratio of 4.33 similar to that determined by X-Ray fluorescence of 4.55. Removal of lead ions from solution decreased from the native (NM-Ca, 0.27(14), NV-Na, 1.50(17) meq/g) compared to the modified zeolites (30 min HCl treated NM-Ca 0.06(9) and NV-Na, 0.41(23) meq/g) and also decreased upon K⁺ ion pretreatment in the HCl modified zeolites.

Keywords: Clinoptilolites, Acid modification, heavy metals, toxic substances, purification, lead removal.

1. Introduction

Natural zeolites, which are composed of hydrated aluminosilicates containing group I and II metals, [1] are an abundant resource [2] with desirable chemical properties for many different applications such as catalysis and ion exchange [3]. Zeolites have a crystalline structure with small voids commonly called pores that act as a site for the zeolite to capture or stabilize different cations or molecules. They have been utilized to remove salinity/sodicity [4], copper [5], Cr⁶⁺ [6], Mn²⁺ [7], heavy metals [8], ammonia [9], phosphorus [10], purify urine [11], zinc [12] from wastewater and also anions such as Cl⁻ and CO₃²⁻ [13]. Zeolites contain cations to stabilize the negative charge in their structure with Na⁺, K⁺, Ca²⁺, and Mg²⁺ being the four most common with others possible [14]. While it is possible to synthesize a single phase of clinoptilolite, [15] as much as 4.75 mg Fe/g of Mexican natural zeolite consisting of clinoptilolite, mordenite, and feldspar phases was reported [16].

During the ion exchange process, zeolites absorb toxic metal ions dissolved in solutions into their pores while releasing the other cations present in the structure into the solutions. Thus, water contaminated with Pb²⁺ ions, which are toxic to humans, could be made safe by stirring with a zeolite to remove the Pb²⁺ ions from the solution. The Pb²⁺

ions would be contained inside the zeolite and could be easily filtered off and the Na^+ ion that was previously in the zeolite would now be dissolved in the water rendering it safer for human consumption [17].

We had recently obtained samples of four naturally occurring zeolites which were of the chabazite and clinoptilolite (based on $\text{Si:Al} \geq 4.0$ [18]) varieties. The chabazite form has been explored for its unusual composition [19] and chemical upgrading, [20], and the clinoptilolite zeolite has been studied for various membrane applications [21-23]. Additionally, both chabazite and clinoptilolite were subjected to treatment with base and applied for Pb^{2+} and Cd^{2+} removal [24]. We decided, based on a report of chemical etching on a glass surface using HCl [25], to explore if modification under acidic conditions while maintaining structural integrity was possible and what impact this would have on their properties and potential use in remediation. A report dealing with the treatment of naturally occurring clinoptilolites in Cuba using 0.6 M HCl discovered that milder forms of acid treatment were required as higher concentrations led to the decomposition of the zeolites [26]. We discovered that treatment with concentrated HCl removes metal ions from the pores leaving the silicon framework intact with the clinoptilolite variety whereas the chabazite ones became amorphous. Structures were assessed on the bases of solid-state ^{29}Si and ^{27}Al NMR, BET measurements, SEM images, and powder X-ray fluorescence and diffraction. Lead removal studies on the clinoptilolite samples suggested differing capacities between the two samples after calcination and deterioration of Pb^{2+} storage capacity upon modification.

2. Materials and Methods

2.1. Materials:

The zeolites were generously donated from St Cloud Mining Company and consisted of St Cloud Mining Bowie chabazite (AZLB-Na, -325 mesh), St Cloud Mining Bowie chabazite (AZLB-Ca, -325 mesh), St Cloud Winston clinoptilolite (NM-Ca, -325 mesh), and St Cloud Mining Ash Meadows clinoptilolite (NV-Na, -325 mesh) where AZLB =Arizona Land Basin, NM = New Mexico, NV = Nevada, Na is the dominant cation, Ca is the dominant cation. HCl (12.1M) and HNO_3 (15.6M) acids were obtained from Fisher. Lead nitrate was obtained from Mallinckrodt Chemical Works.

2.2. Zeolite Modifications:

2.2.1 Calcined Zeolites

The calcined zeolite samples were obtained by heating the zeolites at 550°C for 5 hours under air. After cooling the zeolite, the samples were stored in a desiccator to prevent the absorption of water.

2.2.2 Hydrochloric Acid Treated Zeolites

The HCl acid-treated samples were prepared by refluxing a solution of the acid and zeolite at a ratio of 10 mL of concentrated HCl per gram of zeolite. This was based on a procedural modification from the literature [25] and the samples were placed in an oil bath for 10, 20, 30, or 40 minutes and, upon removal, allowed to cool for 20 minutes. The zeolite was quickly filtered off after cooling and washed with water 3 times at a ratio of 5 mL per gram of zeolite initially used. The zeolite was dried overnight in an oven at 70 °C and then calcined at 550 °C in a flow of air for 5 hours. After cooling, the zeolite was stored in a desiccator to prevent the absorption of water.

2.3 X-ray Diffraction:

X-ray diffraction spectra of the zeolites were collected using a Scintag XDS 2000 Diffractometer (Scintag Division of Thermo Dearborn, Michigan) using a copper target to generate X-rays and a graphite monochromator with a scan range of 5-60° 2θ , a step size of 0.020°, a count time of 0.600 seconds, and a step scan rate of 2.0 deg/min. The samples were packed into an aluminum sample plate of dimensions of 30 mm wide by 90 mm long by 8 mm depth.

The data was analyzed using DMSNT v 1.37 (1994-1998) Scintag Inc. (Division of Thermo Dearborn, Michigan). The spectra were background-subtracted using a manual spline curve fit. Sample phase identification was conducted using QualX2 [27] after the raw data was transformed using PowDLL [28].

2.4 Energy Dispersive Spectroscopy:

EDS/XRF was performed to obtain an elemental composition of the zeolites using a Xenemetrix EX-6600 EDS machine (Migdal HaEmek, Israel) with a rhodium target to generate the X-Rays. Samples were prepared by mixing the zeolite with corn starch at a ratio of 4:1 weight zeolite: corn starch. The mixture was added to an aluminum cup with a diameter of 3 cm and a depth of 0.75 cm. Once packed by hand pressure, the cup was loaded into a hydraulic press and pressure applied for 1 minute up to 700 psi, once reached the sample was held for 1 minute at 700 psi and then for 1 minute the pressure was released.

2.5 Surface Area Analysis:

Surface area analysis was performed using an ASAP 2020 machine made by Micrometrics (Norcross, Georgia). The program used for the analysis was the "5-point BET Analysis" program supplied by the manufacturer. Some modifications were required and consisted of adding parameters from the standard micropore analysis program (from the manufacturer) to the 5 Point BET Program. The samples were degassed at 350 °C at 1 mm Hg for 4 hours and backfilled with nitrogen gas. The BET analysis was performed using nitrogen gas and the micropore analysis was performed using helium gas. Calibration of the machine was checked by running a standard supplied by Micrometrics.

2.6 Lead Removal Studies:

An analysis of the amount of lead absorbed or adsorbed by the zeolite was performed using a Buck Scientific Model 200A atomic absorption spectrometer. A Fisher hollow cathode tube for lead analysis was used at an operating current of 10 mA. The detector was set to a wavelength of 283.3 nm with a slit width of 0.7 nm.

A 335 mg/L concentrated lead nitrate solution was made using water with a pH of 4.5 which was adjusted using HNO₃ acid. 0.250 grams of previously dried zeolite was added to 150 mL of the 335 ppm lead nitrate solution and stirred for 5 days at room temperature [29]. After 5 days the solution was centrifuged, the sample was diluted and analysis was performed on the AAS.

2.7 NMR Study of Zeolite:

²⁷Al MAS and ²⁹Si MAS NMR analyses of calcined NV-Na and 30 min HCl NV-Na were performed at ambient temperature on a Varian Infinity-Plus NMR spectrometer equipped with a 6 mm MAS broadband probe operating at 79.41 MHz for ²⁹Si, 104.2 MHz for ²⁷Al, and 399.75 MHz for ¹H. Samples were spun at the magic angle at 4 kHz. A standard one-pulse was used for all experiments. The ²⁹Si pulse width was 4 μ s, the pulse delay was 120 s, the acquisition length was 20.5 ms, and between 650-700 scans were collected. Exponential multiplication of 100 Hz was used before the Fourier transform. Chemical shifts were referenced against an external sample of talc at -98.1 ppm relative to TMS (tetramethylsilane) at 0 ppm. The ²⁷Al pulse width was 1 μ s, the pulse delay was 0.2 s, the acquisition length was 2.1 ms, and between 8,000-10,000 scans were collected. Exponential multiplication of 100 Hz was used prior to the Fourier transform. Chemical shifts were referenced against an external sample of 1M Al(NO₃)₃ at 0.0 ppm.

2.8 Scanning Electron Microscopy

SEMs were performed on a Hitachi S4700 Scanning Electron Microscope at a voltage of 15-20 kV and 10-20 μ A.

2.9 ATR-FTIR

FTIR was performed on a PerkinElmer Spectrum one (neat samples) with a Perkin Elmer universal ATR sampling attachment.

3. Results and Discussion

3.1. X-Ray Diffraction

3.1.1. Initial Phase Assignment

The spectra obtained for AZLB-Ca, Fig. 1 and AZLB-Na, Fig. 2 suggests the presence of chabazite if one compares the patterns to that obtained from simulations [30] of single-crystal X-ray data [21]. In particular, we note the presence of the intense reflections for Miller indices (1 0 0) and (3 1 1) at 2 θ of 9.40° and 30.40° respectively which are ascribed to chabazite [30]. These suggest that the samples were dominantly chabazite, however differing ratios of erionite and AlPO₄-D were also evident in the samples [30,31]. Interestingly, no phases indicative of clinoptilolite, heulandite, or alpha quartz were observed in either sample AZLB-Ca or AZLB-Na, Figs. 1 and 2 respectively.

The X-ray powder spectra for the clinoptilolite samples, NV-Na Fig. 3 and NM-Ca Fig. 4 also contained large differences. Evidence for clinoptilolites is in the presence of reflections at 9.88°, 11.19° and 22.49° in 2 θ ascribable to the (0 2 0), (2 0 0) and (3 3 0) Miller indices respectively [30,32,33]. In the case of the calcined NV-Na sample (Fig. 3) signals for these peaks are quite intense and the sample appears to be quite pure. There was a match for clinoptilolite-Na (card [00-900-1391]) at a FoM of 0.75 determined using QualX2 [27]. Raw data from the diffractometer were converted with PowDRL [28] for use with the QualX2 program. In the case of NM-Ca (Fig. 4), the most intense peak is located at about a 2 θ of 26.6° and the program QualX2 [27] could not find a match to clinoptilolite. This is probably because this calcined NM-Ca sample is mostly alpha quartz which has its most intense reflection at a 2 θ of 26.65° due to the (1 0 1) Miller phase [34]. There is some evidence of clinoptilolite in the sample judging by small peaks at the 2 θ angles mentioned above but it is clearly not the dominant constituent. No chabazite or erionite species were observed in either sample NV-Na or NM-Ca.

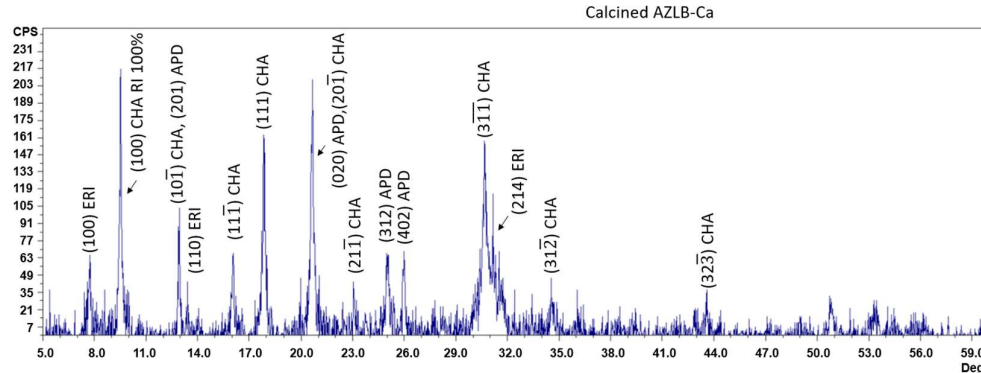


Figure 1. The XRD pattern of calcined AZLB-Ca. Abbreviations ERI=erionite, CHA=chabazite, APD=AlPO₄-D , RI=Relative intensity. Identification based on data in reference [30].

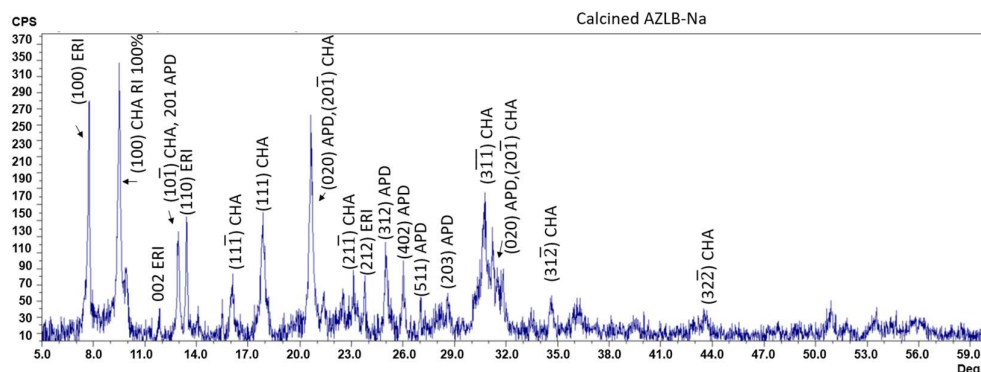


Figure 2. The XRD pattern of calcined AZLB-Na. Abbreviations ERI=erionite, CHA=chabazite, APD=AlPO₄-D, RI=Relative intensity. Identification based on data in reference [30].

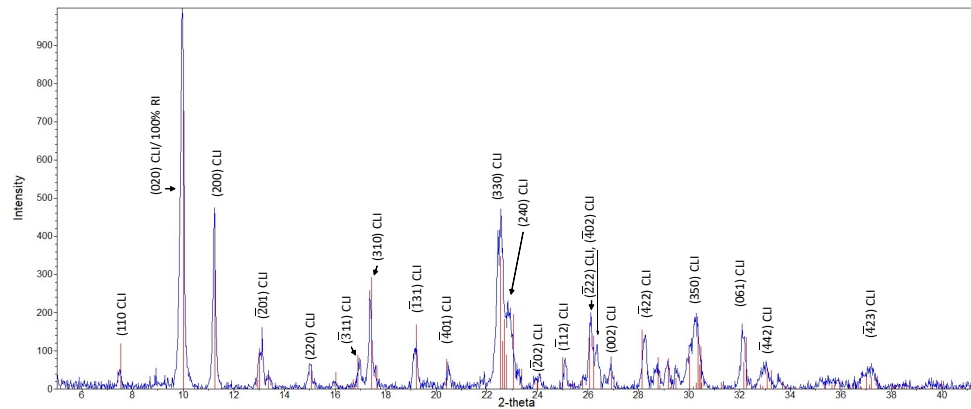


Figure 3. The XRD pattern of calcined NV-Na. Abbreviations, CLI = clinoptilolite, RI= relative intensity. Identification based on data in reference [30]. Solid vertical lines represent card [00-900-1391] clinoptilolite-Na at a FoM of 0.75 as determined using QualX [27]. Raw data converted with PowDRL [28].

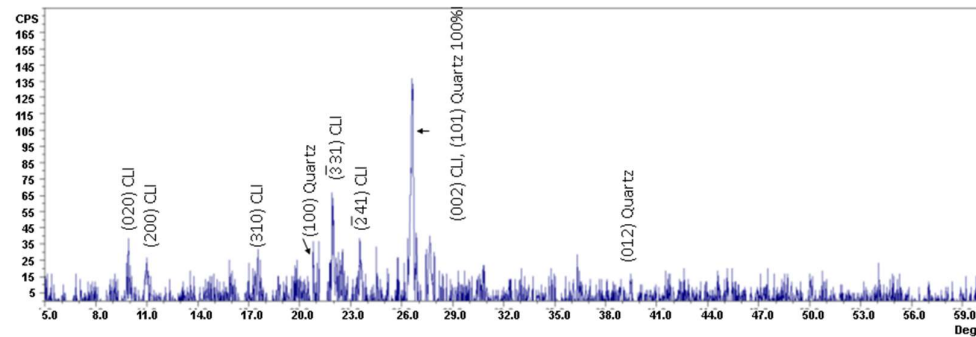


Figure 4. The XRD pattern of calcined NM-Ca. Abbreviations, CLI = clinoptilolite, RI=relative intensity. Identification based on data in reference [30].

The AZLB-Na and AZLB-Ca zeolites lost all crystallinity when boiled in HCl acid for 30 minutes which is demonstrated by the loss of all sharp reflections and the spectra appearing as broad bumps (Figs. 5 and 6) as a result of random scattering due to an amorphous material. In contrast, the NV-Na and NM-Ca zeolites did not lose all crystallinity during the boiling process in HCl acid (Figs. 7 and 8, respectively). This is conclusive evidence of the instability of these chabazites subjected to HCl modification and the inherent stability of the clinoptilolites as evident in the 30 min HCl NV-Na, Fig. 7, card [00-900-1393] clinoptilolite-Na at a FoM of 0.66, and 30 min HCl NM-Ca, Fig. 8, card [00-901-4410] boggsite [35] of formula Ca_{3.4}O_{70.76}Si₂₄ at a FoM of 0.77, both determined using QualX2 [27]. In particular, NM-Ca registered the least change possible because it is mostly composed of alpha quartz, Fig. 8.

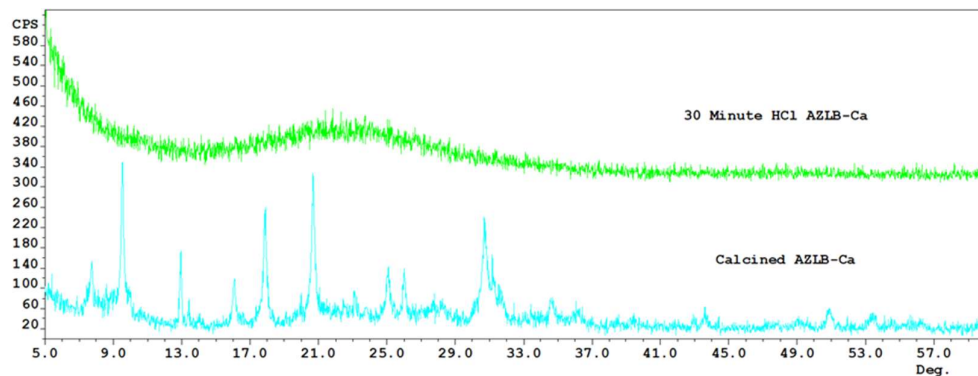


Figure 5. The XRD patterns of calcined AZLB-Ca and 30 minute HCl AZLB-Ca.

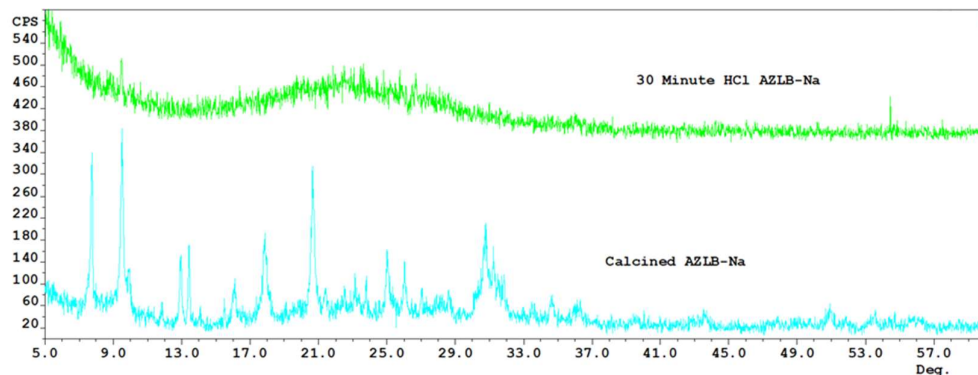


Figure 6. The XRD patterns of calcined AZLB-Na and 30 minute HCl AZLB-Na.

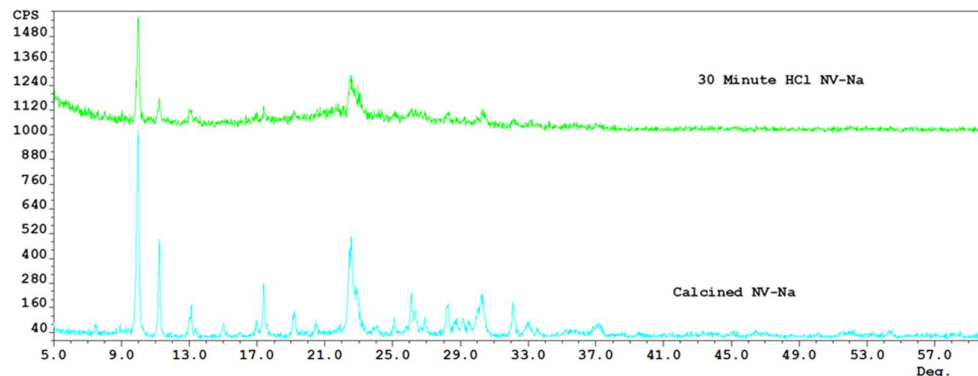


Figure 7. The XRD patterns of Calcined NV-Na and the 30 minute HCl NV-Na.

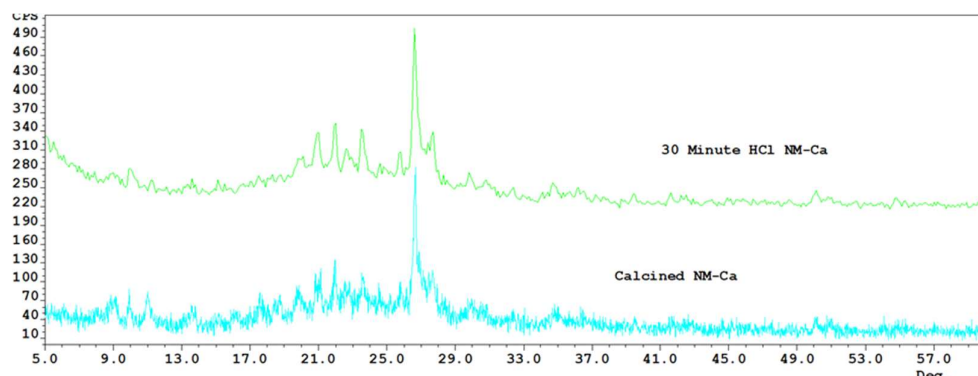


Figure 8. The XRD patterns of Calcined NM-Ca and 30 minute HCl NM-Ca.

3.2 Surface Area Analysis

Based on the fact that the chabazite samples lost crystallinity upon treatment with conc. HCl, we only conducted surface area analyses on the clinoptilolite samples. Thus NM-Ca and NV-Na were both subjected to boiling concentrated HCl acid for a varying amount of time from 10-40 minutes as listed with the surface area analysis results (Table 1). This indicated that 30-minute etching of the zeolite produced the highest surface area with 40-minute etching resulting in a decrease in the surface area which is likely due to the acid collapsing some of the crystalline structure. Therefore, in this case, the optimum time for boiling the clinoptilolite zeolite in HCl acid is 30 minutes. In the case of NV-Na, the surface area increased from 19 to 158 m²/g and the pore volume increased from 0.04 cm³/g to 0.12 cm³/g. The NM-Ca increased in surface area from 20 to 111 m²/g and the pore volume increased from 0.04 to 0.10 cm³/g.

The values for the micropore, mesopore, and external surface areas provide valuable insight into what is happening during the etching process, Tables 1 and 2. There is a dramatic increase in micropore area of the HCl acid-etched zeolites, 4.800 to 94.99 m²/g for calcined NV-Na to 30 min HCl NV-Na and 2.730 to 55.15 m²/g for calcined NM-Ca to 30 min HCl NM-Ca, suggesting that either new micropores are forming and/or the existing micropores are being deepened increasing their surface area. In the case of the calcined NM-Ca sample versus the 10-Min HCl NM-Ca sample, Table 2, the 10 min HCl NM-Ca sample has a smaller average micropore diameter going from 4.584 to 4.388 Å and this likely represents new micropores being formed thus lowering the average value for the micropore diameter. The 30 min HCl NM-Ca sample seems to reach a maximum average micropore diameter of 4.597 Å before declining in the 40 min HCl NM-Ca sample to 4.588 Å which is probably due to the crystallinity of the zeolite collapsing based on the loss of surface area of the sample, see Table 1. In contrast, NV-Na appears less stable to HCl treatment and the average micropore diameter increases from 4.586 to 4.600 Å for calcined NV-Na to 30 min HCl NV-Na respectively.

In the case of mesopores, calcined NV-Na has a value of 91.00 Å which decreases to 31.06 Å in the 10 min HCl NV-Na sample. This is attributable to the formation of new mesopores thus lowering the average diameter of mesopores. The same trend is observed with the calcined NM-Ca sample which has an initial average mesopore diameter of 93.71 Å (calcined NM-Ca) and changes to 40.31 Å (10 min HCl NM-Ca) sample. In the case of the NM-Ca zeolite, the average mesopore diameter continues to become lower with longer treatment in HCl acid, however, the NV-Na zeolite reaches equilibrium around a 32 Å average mesopore diameter (Table 2).

Table 1. The surface area analysis measurements for calcined and HCl etched zeolites.

Sample	5 Point BET Surface	Pore Volume	Micropore Volume	Micropore	External Surface
	area (m ² /g)	(cm ³ /g)	(cm ³ /g)	Area (m ² /g)	Area (m ² /g)
NV-Na Calcined	19.0(4)	0.04	0.002	4.8	14.23
10 min HCl NV-Na	147(6)	0.11	0.049	93.28	52.05
20 min HCl NV-Na	141(6)	0.11	0.043	81.43	59.87
30 Min HCl NV-Na	158(7)	0.12	0.051	94.99	63.15
40 min HCl NV-Na	138(6)	0.11	0.041	75.06	63.49
NM-Ca Calcined	20.0(1)	0.04	0.001	2.73	17.27
10 min HCl NM-Ca	82.0(3)	0.08	0.021	38.71	43.36
20 min HCl NM-Ca	89.0(3)	0.08	0.022	41.61	47.75
30 min HCl NM-Ca	111(4)	0.1	0.029	55.15	56.22

40 min HCl NM-Ca	101(4)	0.08	0.028	53.53	48.28
------------------	--------	------	-------	-------	-------

Table 2. The average mesopore and micropore diameter.

Sample	Average Micropore Diameter (Å)	Average Mesopore Diameter (Å)
NV-Na Calcined	4.586	91.00
10 min HCl NV-Na	4.597	31.06
20 min HCl NV-Na	4.591	32.44
30 Min HCl NV-Na	4.600	31.72
40 min HCl NV-Na	4.598	32.95
NM-Ca Calcined	4.584	93.71
10 min HCl NM-Ca	4.388	40.31
20 min HCl NM-Ca	4.584	39.62
30 min HCl NM-Ca	4.597	36.36
40 min HCl NM-Ca	4.588	34.63

3.3 X-Ray Fluorescence/EDS

The NM-Ca zeolite has a much greater mole percentage concentration of Ca (6.31%) compared to that for NV-Na (1.14%) while containing less Na, (0.10 to 0.25 respectively), clearly justifying the label, Table 3. There is also more Fe in NM-Ca compared to NV-Na (2.67 to 0.79% respectively) and correspondingly less Si (76.26 to 84.36% respectively). The X-ray fluorescence data results in Table 3 show by way of the reduction in molar percentage concentrations that etching the zeolites in concentrated HCl acid effectively removes sodium, calcium, potassium, magnesium, iron, and aluminum while it appears the silicon remained mostly unaffected. Table 4 lists the weight percentage data supplied by the

Table 3. The XRF data for zeolites in mole %.

Experimental Run	Na	Ca	K	Mg	Fe	Al	Si	P	Si:Al ₂ Ratio
NV-Na	0.25±0.08	1.14±0.04	3.34±0.08	0.30±0.08	0.79±0.01	9.27±0.24	84.36±0.70	0.442±0.08	4.55
30 Min NV-Na	0.02±0.04	0.05±0.01	0.30±0.02	0.16±0.04	0.04±0.002	4.16±0.11	95.04±0.49	0.17±0.03	11.42
NM-Ca	0.10±0.04	6.31±0.11	4.29±0.10	0.52±0.05	2.67±0.04	9.51±0.17	76.26±0.46	0.27±0.04	4.01
30 Min NM-Ca	0.04±0.04	0.42±0.04	2.54±0.08	0.17±0.05	0.07±0.002	4.71±0.13	91.83±0.56	0.17±0.04	9.75

manufacturer [36] and that obtained by converting the molar percentages in Table 3 to weight percentages. This requires the assumption that only the ions listed in Table 3 were present and that they are present in the zeolite in the oxide form indicated in the table. Additionally, XRF is not good at determining very low concentrations. However, there are large differences in the weight percentages between our determinations and those determined by the manufacturer. This may well be due to natural variation in the samples used in the studies. Our determinations of the concentrations of Al₂O₃ would appear to be much lower whereas those for SiO₂ are higher compared to those listed by the manufacturer. However, this does correlate with the X-ray powder diffraction pattern where quartz was found in NM-Ca, Fig. 8. On this basis, NV-Na is composed mostly of K₂O, Al₂O₃, and SiO₂ in contrast to NM-Ca where CaO, K₂O, Fe₂O₃, Al₂O₃, and SiO₂ are the major contributors. This calculation allows for a stoichiometric formula for NV-Na of [Na₂O]_{0.01}[CaO]_{0.11}[K₂O]_{0.27}[MgO]_{0.02}[Fe₂O₃]_{0.11}[P₂O₅]_{0.05}[Al₂O₃]_{0.80}[SiO₂]_{8.63} and NM-Ca of [CaO]_{0.60}[K₂O]_{0.34}[MgO]_{0.04}[Fe₂O₃]_{0.36}[Al₂O₃]_{0.83}[SiO₂]_{7.79}.

Table 4. The weight percentages from our calculated data and that of the manufacturer.

Experimental Run	NV-Na			NM-Ca		
	mole %	Formula	Calculated	Manufacturer	Calculated	Manufacturer
	Na	Na ₂ O	Wt%	Wt % ^a	Wt%	Wt % ^a
	0.10	Na ₂ O	0.13	3.5	0.05	0.3

Ca	6.31	CaO	1.09	0.8	6.02	3.4
K	4.29	K ₂ O	2.68	3.8	3.44	3.2
Mg	0.52	MgO	0.21	0.4	0.36	1.4
Fe	2.67	Fe ₂ O ₃	1.07	0.7	3.63	1.6
Al	9.51	Al ₂ O ₃	8.04	11.9	8.25	11.9
Si	76.26	SiO ₂	86.25	69.1	77.94	64.9
P	0.27	P ₂ O ₅	0.53		0.33	>0.05
		MnO		0.02		
		TiO ₂		0.1		
Total			100	90.32	100	86.7

^areference [36]

3.4 Lead Removal Study

We were interested in comparing the lead absorption and/or adsorption capacities between the calcined material and the 30 min HCl modified clinoptilolites which had more micropores and a larger surface area. First, AZLB-Na and AZLB-Ca removed 2.05(27) and 2.00(11) meq/g of Pb²⁺ and this was slightly more than the removal with the clinoptilolites as evident in Table 5. This difference, i.e., better removal with chabazites than clinoptilolites was previously noted [24]. Two other natural clinoptilolites report an ion exchange of 0.730 meq/g Pb²⁺ [37], and 0.433 meq/g Pb²⁺ [38]. NV-Na calcined is significantly better at the ion exchange of Pb²⁺ than these natural clinoptilolites at 1.50±0.17 meq/g, Table 5. NM-Ca, 30 min HCl NV-Na, and 30 min HCl NM-Ca s are not efficient at the ion exchange of Pb²⁺ with ion exchanges of 0.27, 0.41, and 0.06 respectively, Table 5.

The results of this lead removal study prove that treating the zeolite in HCl acid decreases the ability of the zeolite to remove lead ions from the solution. Theoretically, if the removal of lead was based on ion exchange, the Pb²⁺ ion would likely exchange with K⁺ due to the radius of Pb²⁺ being 133 pm versus K⁺ having a radius of 137 pm [39]. However, if lead ions are exchanged solely with K⁺ ions, we would have expected NM-Ca to have a higher rate of removal than NV-Na. The increase in uptake by NV-Na may be attributed to the fact that it contains less quartz than NM-Ca, thus a more clinoptilolite structure, as was evident in the X-ray powder diffraction spectra, Figs. 3 and 4.

Table 5. The Pb²⁺ removal by the zeolites at a time of 5 days at 35°C. [13]

Sample	Meq/g of Pb ²⁺ (3 samples)
AZLB-Na	2.05 (27)
AZLB-Ca	2.00(11)
NV-Na calcined	1.50(17)
NM-Ca calcined	0.27(14)
30 Min HCl NV-Na	0.41(23)
30 Min HCl NM-Ca	0.06(9)

In order to increase the lead ion uptake, the zeolites were stirred in a 1M KCl solution at 25°C for 5 days. They were then filtered and washed with water until the filtrate was clear of chloride ions which was monitored by tests with silver nitrate solution [40]. After drying and calcining at 550 °C for 5 hours, these treated zeolites were tested similarly for their ability to remove lead ions from polluted water.

Table 6. The Pb²⁺ removal by the K⁺ charged zeolites at a time of 5 days at 35°C.

Sample	Meq/g of Pb ²⁺ (3 samples)
K ⁺ charged NV-Na	0.84(5)
K ⁺ charged NM-Ca	0.34(3)
K ⁺ charged 30 Min HCl NV-Na	0.22(5)
K ⁺ charged 30 Min HCl NM-Ca	0.07(9)

The results listed in Table 6 show that charging NV-Na with KCl decreased its ability to remove lead as there was a significant decrease in the quantities removed, 1.50(17) for NV-Na calcined to 0.84(5) meq/g for the K⁺ charged sample. There were no significant differences with the other zeolites as this method did not have high enough precision as is evident in the data in Tables 5 and 6. However, charging these zeolites with potassium ions by stirring in a potassium chloride solution was ineffective at increasing the zeolite's ability to remove Pb²⁺ ions from the solution. It is also possible given the high percentage concentration of Si in the two zeolites, removal of the Fe³⁺ and Al³⁺ ions result in a more electrically neutral species thus reducing the capacity for ion exchange.

3.5 ²⁷Al NMR

Aluminum NMR is very sensitive to the geometry with 6-coordinate species resonating around 4-11 ppm and 4-coordinate downfield in the range 55-66 ppm depending on the nature of the aluminosilicate species [41]. Only one signal at 55 ppm belonging to tetrahedral aluminum species was evident in the ²⁷Al spectrum of a clinoptilolite found in Cuba [26]. As is evident in Fig. 9, which displays the ²⁷Al NMR of the calcined NV-Na sample, the Al in that sample is composed mainly of 4-coordinate Al species as the spectrum consists mainly of a large single resonance at 54.49 ppm. A much smaller quantity is in the octahedral conformation which corresponds to the peak at 2.60 ppm. Applying a framework equation [41] which equates the position of the ²⁷Al isotropic chemical shift to the angles on the Al (i.e., $\delta_{Al} = 132 - (0.5 \cdot \angle Al-O-Si)$) would suggest a mean $\angle Al-O-Si$ of 155°. However, this derivation is not valid for zeolites with a high percentage of Si as other factors also pertain [42].

Subjecting the zeolite to HCl resulted in changes in the ²⁷Al NMR spectrum as evident in Fig. 10. The peak for the 4-coordinate species in calcined NV-Na shifts from 54.99 to a broad peak with peaks at 53.96 and 59.64 ppm for the 30 min HCl NV-Na. Additionally, there is a slight shift in the octahedral resonance from 2.60 to 2.03 ppm. This indicates that the ratio of tetrahedral to octahedral aluminum has changed, however, it is unknown whether this is due to conversion or the dissolution of one of the forms following HCl treatment [19].

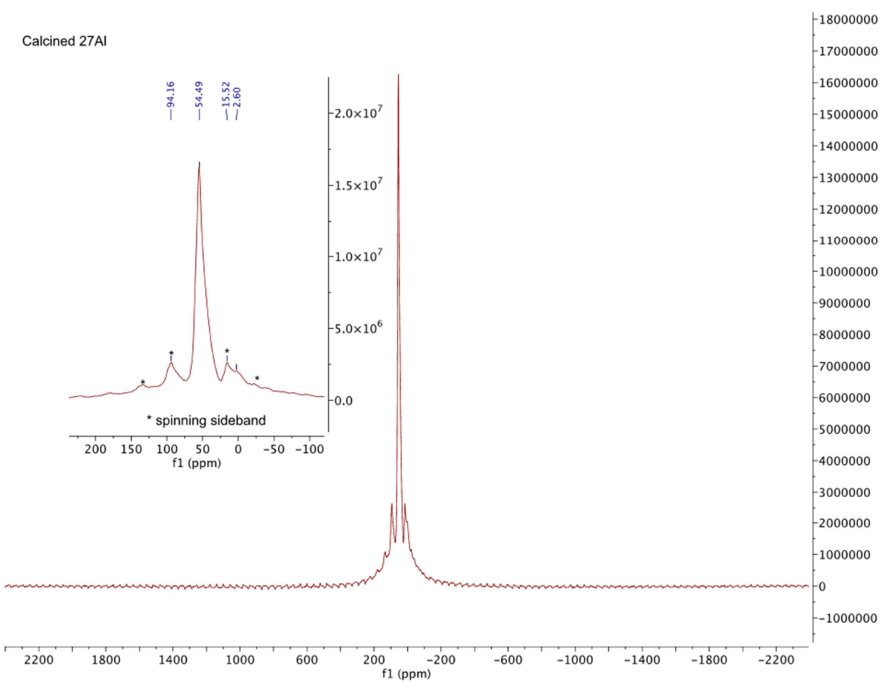


Figure 9. The ^{27}Al NMR of calcined NV-Na externally referenced to 1M $\text{Al}(\text{NO}_3)_3$ at 0.0 ppm.

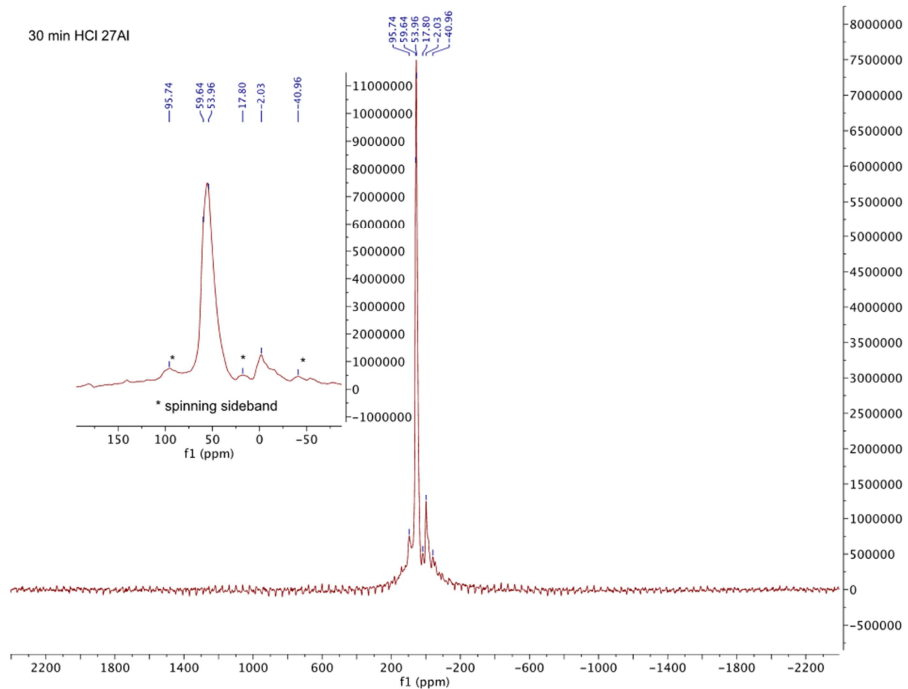


Figure 10. The ^{27}Al NMR of 30 min HCl NV-Na externally referenced to 1M $\text{Al}(\text{NO}_3)_3$ at 0.0 ppm.

3.6 ^{29}Si MAS NMR

3.6.1 Calcined NV-Na

The ^{29}Si NMR spectrum of clinoptilolite has been reported to consist of peaks at -112.8, -106.9, and -100.6 ppm with the peak at -106.9 having the highest intensity [43]. The spectrum for calcined NV-Na contains many signals as listed in Fig. 11, but the one with the most area occurs at -106.02 ppm (27.12%). Peaks at -112.14 (13.46%) and -100.1 (23.43%) ppm are also obtained and these are probably from the clinoptilolite regions within calcined NV-Na. Peaks at -95.99 (19.56%), -101.11 (2.48%), -108.58 (13.90%) ppm are also evident in the deconvoluted analysis, Fig. 10. The peak at -95.99 ppm may be either due to SiOH and $\text{Si}(\text{OH})_2$ groups as Si resonances for these groups lie in this range [43] or related to the presence of Fe^{3+} complexes rather than Al^{3+} [26]. Studies on a natural clinoptilolite from Cuba reported peaks and area percentages of -94.90 (5.7%), -97.8 (2.3%), -100.90 (34%), -106.90 (45.3%) and -112.70 (13.7%) [26]. These peaks are very close in position and area to that ascribed to a heulandite zeolite which has the following peaks and areas, -93.44 (4.25%), -98.44 (31.26%), -104.63 (56.11%), and -111.41 (8.37%) [44]. However, in our NV-Na sample, the peaks at -101.11 (2.48%) and -108.58 (13.90%) are probably due to impurities with the one at -108.58 ppm possibly due to regions of pure $(\text{SiO}_2)_n$ [45].

The Si:Al ratio was calculated from the ^{29}Si MAS NMR data using Equation 1 [43].

$$\frac{\text{Si}}{\text{Al}} = \frac{\sum_0^4 I_{\text{Si}(n\text{Al})}}{\sum_0^4 0.25 * n I_{\text{Si}(n\text{Al})}} \quad (1)$$

In this equation, n represents the number of aluminum atoms connected to silicon through an oxygen bridge, and a value of 4.34 for the Si:Al ratio pertains to justify a mostly clinoptilolite designation.

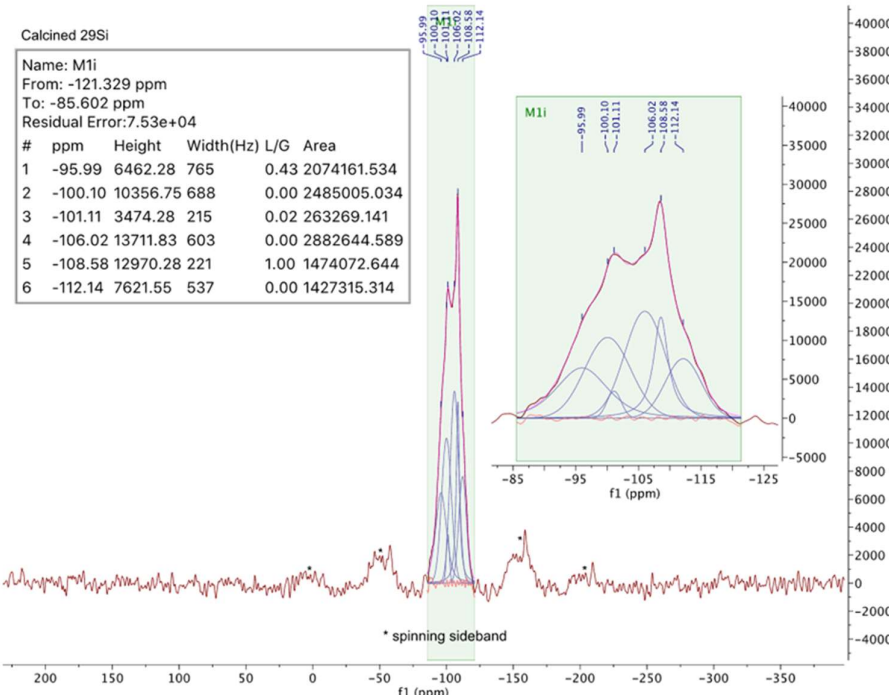


Figure 11. The ^{29}Si NMR spectrum of calcined NV-Na referenced externally to a sample of talc at -98.1 ppm relative to tetramethylsilane (TMS) at 0 ppm. The shaded inset depicts the obtained resonances on top and the deconvoluted components of the fit below.

3.6.2 30 min HCl NV-Na

There are dramatic changes to the ^{29}Si NMR spectrum of the 30 min HCl NV-Na, Fig. 12, compared to NV-Na, Fig. 11. A peak (ppm) and area percentage profile of -91.13 (1.83%), -94.01 (1.97%), -97.51 (9.25%), -102.81 (22.40%), -108.37 (39.36%) and -112.33 (25.19%) is obtained. Thus we have the disappearance of the intense clinoptilolite peak at -106.02 present in NV-Na and an increase in the peak at -108.37 which was ascribed above to $(\text{SiO}_2)_n$ entities. The peaks at -91.13 and -94.01 may be due to SiOH and $\text{Si}(\text{OH})_2$ groups and the peaks at -97.51 and -102.81 ppm correspond to silicon being connected to either 1 or 2 aluminum atoms via oxygen atom bridges [43]. As the nature of this modified zeolite is not known precisely, the Si:Al ratio cannot be assessed.

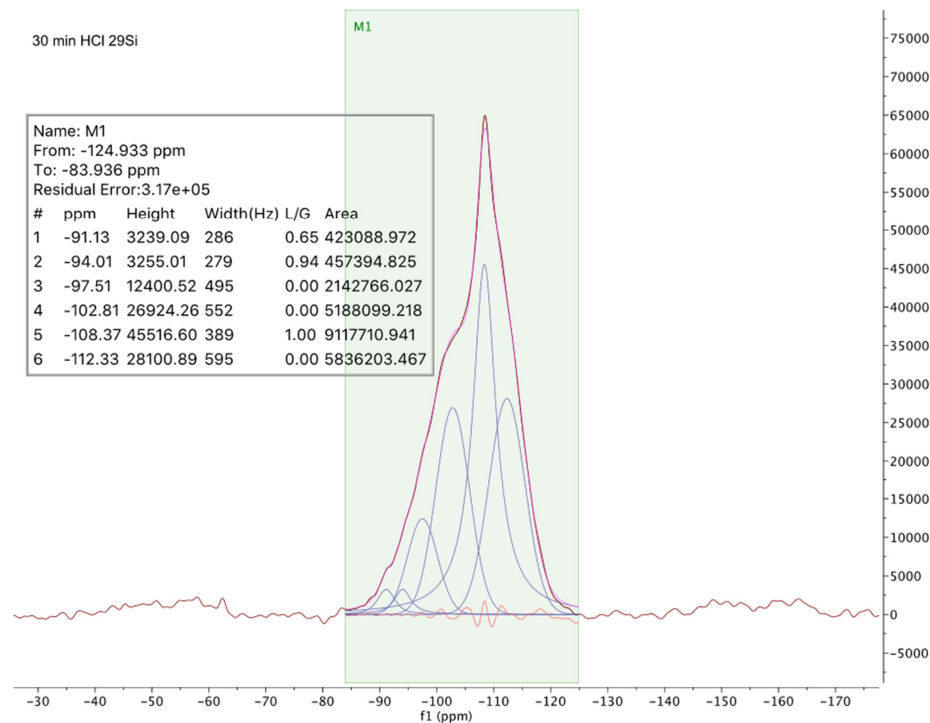


Figure 12. The ^{29}Si NMR spectrum of 30 min HCl NV-Na referenced externally to a sample of talc at -98.1 ppm relative to TMS at 0 ppm. The resonances on top are from the sample and the deconvoluted components of the fit are below.

3.7 SEM

Scanning electron micrographs of calcined NV-Na and 30 min HCl NV-Na were obtained as presented in Fig. 13. The overall morphology of calcined NV-Na looks smoother than those published at an equal magnification (i.e., 10 μm) and somewhat larger, approx. 20 μm compared to 5 μm [46]. HCl treatment results in a much less “smooth” surface comparing the images in Fig. 13 (b) for calcined NV-Na and (e) for 30 min HCl NV-Na and there appear to be many more voids which correlates positively with the increase in surface area measurements from the BET calculations. The 5 μm images for the samples consist of smooth surfaces albeit with smaller particle sizes for the 30 min HCl NV-Na.

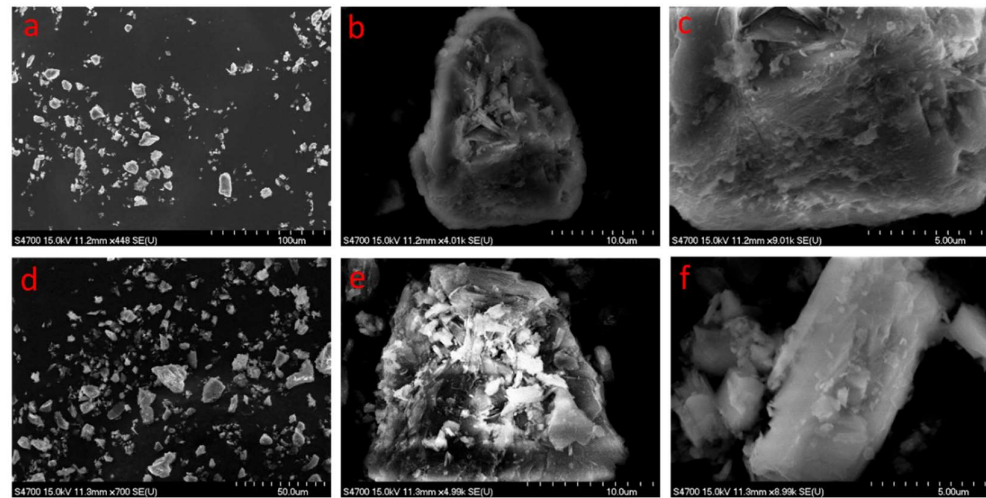


Figure 13. The SEM images of calcined NV-Na at a $100\mu\text{m}$ scale (a), a $10\mu\text{m}$ scale (b), and a $5\mu\text{m}$ scale (c) and that of 30 min HCl NV-Na at a $50\mu\text{m}$ scale (d), a $10\mu\text{m}$ scale, (e), and a $5\mu\text{m}$ scale (f).

3.8 FTIR

The FTIR spectra for the calcined and HCl-modified clinoptilolites are displayed in Fig. 14. All contain a small absorption around 1650 cm^{-1} which has been ascribed to a deformation vibration of residual water bound up inside of the zeolite [47]. The very large broad absorption is due to stretches of the Si-O or Al-O bonds of a tetrahedral nature in the zeolite. It is noteworthy that the center of this absorption shifts from 1024 to 1071 cm^{-1} for the calcined NV-Na to 30 min HCl NV-Na. Quartz is known to have a large absorption around 1088 cm^{-1} [48] and the fact that this peak for the 30 min HCl NV-Na occurs at 1071 cm^{-1} would suggest that most of the non-Si elements were removed in the HCl treatment, leaving behind essentially porous quartz. The peaks around 795 cm^{-1} are due to the symmetric stretch of Si-O or Al-O bonds of a tetrahedral nature of the zeolite [49]. Finally, the peak that appears in calcined NV-Na at 672 cm^{-1} is indicative of an octahedral species most likely aluminum or iron [47].

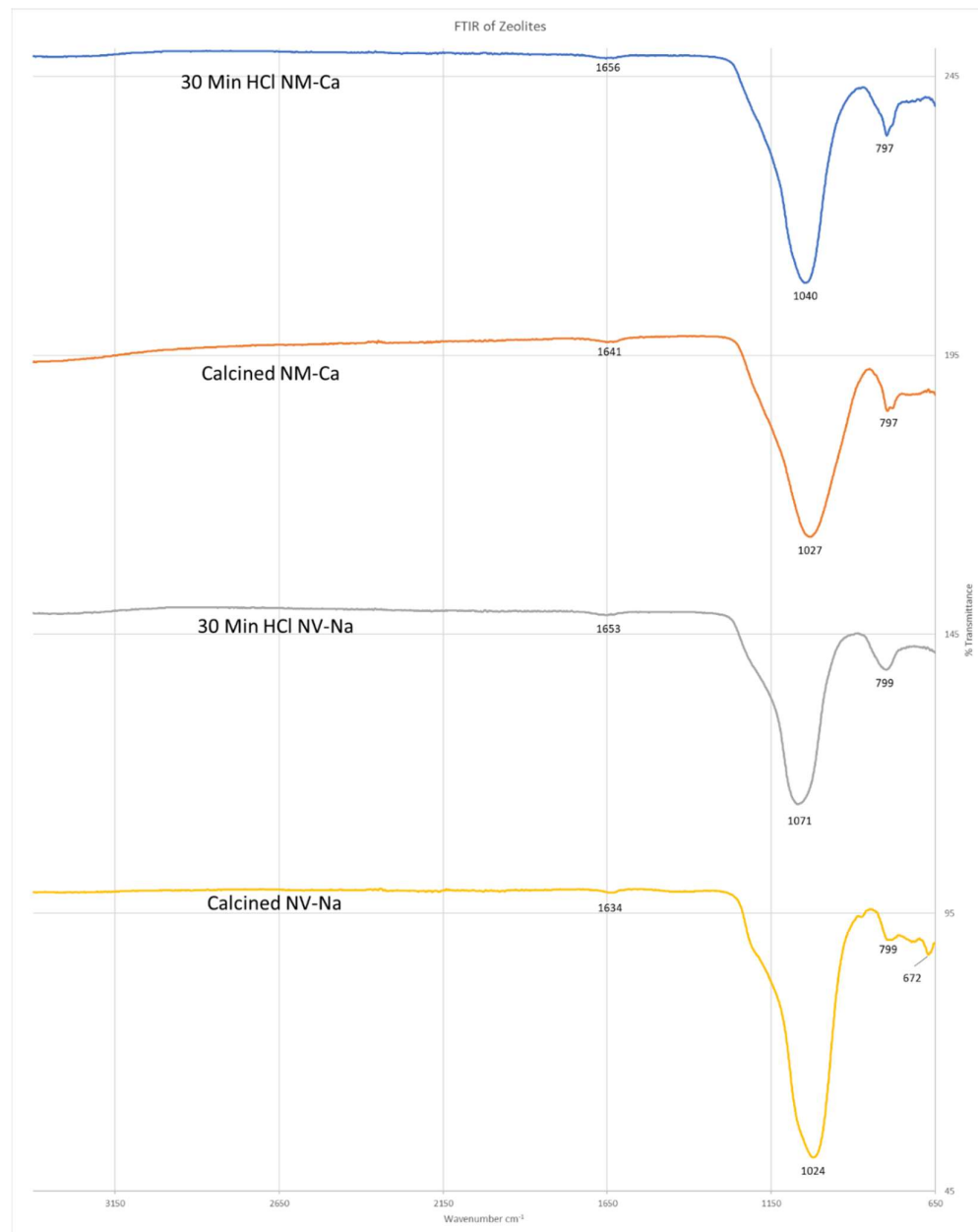


Figure 14. The FTIR spectra of Calcined NV-Na, 30 min HCl NV-Na, Calcined NM-Ca, and 30 min HCl NM-Ca.

4. Conclusions

Of the four zeolites studied AZLB-Ca, AZLB-Na, NV-Na, and NM-Ca, the two chabazites (AZLB-Na and AZLB-Ca) lost structural integrity after boiling in concentrated HCl acid. These materials lost all crystallinity as is evident by the amorphous pattern generated in the powder X-ray diffraction patterns. Zeolites NV-Na and NM-Ca, which are clinoptilolites, withstood boiling in concentrated HCl acid as can be seen by the remaining sharp peaks in their powder X-ray diffraction spectra. Results from X-ray fluorescence measurements confirmed that concentrated HCl acid was effective at removing aluminum, calcium, magnesium, sodium, potassium, and iron from the framework. These two results suggested that NM-Ca had a higher concentration of quartz impurities than NV-Na. The increase in pore size/ or increase in the number of pores by removing atoms from the structure was confirmed via BET surface area analysis. A lead removal study

performed to determine whether the increase in pore size/ or increase in the number of pores after the acid treatment would result in increased capturing of lead ions, found that the acid treatment decreased the ability of the zeolite to absorb lead ions from the solution. This increase in surface area of the natural zeolites due to the acid treatment was not useful at increasing the cation removal or ion exchange capabilities.

Author Contributions: Conceptualization, R.L.; methodology, R.L., N.N.; formal analysis, N.N., R.L.; investigation, G.H., N.N.; resources, R.L., M.M.; data curation, G.H., N.N.; writing—original draft preparation, N.N., R.L.; writing—review and editing, R.L., N.N., G.H., M.M.; visualization, N.N., R.L.; supervision, R.L.; project administration, R.L., N.N.. All authors have read and agreed to the published version of the manuscript.”

Funding: This research received no external funding.

Acknowledgments: Special thanks to Jared Edwards for obtaining and Professor Tarun Dam for paying for the SEM images, Edward Laitila for assistance with the XRF measurements, and Director Daniel Holmes of the Max T. Rogers NMR Facility at Michigan State University for the solid-state NMR spectra. The zeolites were generously donated by the St. Cloud Mining Company. We thank Michigan Technological University for its support.

Conflicts of Interest: The authors declare no conflict of interest.

References

1. Virta, R.L., Zeolites. *U.S. Geological Survey Minerals Yearbook* **2001**, 1-5.
2. Smith, J.V., Origin and structure of zeolites. *ACS Monogr.* **1976**, *171*, 3-79.
3. Mumpton, F.A., *La roca magica: Uses of natural zeolites in agriculture and industry*. *Proceedings of the National Academy of Sciences* **1999**, *96*, 3463.
4. Wen, J.; Dong, H.; Zeng, G., Application of zeolite in removing salinity/sodicity from wastewater: A review of mechanisms, challenges and opportunities. *J. Cleaner Prod.* **2018**, *197*, 1435-1446.
5. Krstic, V.; Urosevic, T.; Pesovski, B., A review on adsorbents for treatment of water and wastewaters containing copper ions. *Chem. Eng. Sci.* **2018**, *192*, 273-287.
6. Chojnacka, M.; Sobolewska, P.; Petrus, R.; Warchol, J., Cr(vi) sorption on surface-modified natural zeolites. *Przem. Chem.* **2017**, *96*, 332-337.
7. Ates, A.; Akgül, G., Modification of natural zeolite with naoh for removal of manganese in drinking water. *Powder Technol.* **2016**, *287*, 285-291.
8. Zhao, Y., Review of the natural, modified, and synthetic zeolites for heavy metals removal from wastewater. *Environ. Eng. Sci.* **2016**, *33*, 443-454.
9. Wang, K., Method and regeneration of sodium modified zeolites for treatment of ammonia-nitrogen wastewater. *Shuichuli Jishu* **2016**, *42*, 118-120.
10. Shi, H.; Wei, L.; Yan, C.; Li, X., Research progress of phosphorus removal by zeolite in wastewater. *Guangdong Huagong* **2014**, *41*, 165, 169.
11. Regmi, U.; Boyer, T.H., Ammonium and potassium removal from undiluted and diluted hydrolyzed urine using natural zeolites. *Chemosphere* **2021**, *268*, 128849.
12. Zwain, H.M.; Vakili, M.; Dahlan, I., Waste material adsorbents for zinc removal from wastewater: A comprehensive review. *Int. J. Chem. Eng.* **2014**, 347912/347911-347912/347913, 347914 pp.
13. Suhartana; Sukmasari, E.; Azmiyawati, C., Modification of natural zeolite with fe(iii) and its application as adsorbent chloride and carbonate ions. *IOP Conference Series: Materials Science and Engineering* **2018**, *349*, 012075.
14. Armbruster, T.; Gunter, M.E., Crystal structures of natural zeolites. *Reviews in Mineralogy and Geochemistry* **2001**, *45*, 1-67.
15. Ambrozova, P.; Kynicky, J.; Urubek, T.; Nguyen, V.D., Synthesis and modification of clinoptilolite. *Molecules* **2017**, *22*, 1107.

16. Ruíz-Baltazar, A.; Esparza, R.; Gonzalez, M.; Rosas, G.; Pérez, R., Preparation and characterization of natural zeolite modified with iron nanoparticles. *Journal of Nanomaterials* **2015**, *2015*, 364763.

17. Wani, A.L.; Ara, A.; Usmani, J.A., Lead toxicity: A review. *Interdisciplinary toxicology* **2015**, *8*, 55-64.

18. Coombs, D.S.; Alberti, A.; Armbruster, T.; Artioli, G.; Colella, C.; Galli, E.; Grice, J.D.; Liebau, F.; Mandarino, J.A.; Minato, H., *et al.*, Recommended nomenclature for zeolite minerals: Report of the subcommittee on zeolites of the international mineralogical association, commission on new minerals and mineral names. *Can. Mineral.* **1997**, *35*, 1571-1606.

19. Thrush, K.A.; Kuznicki, S.M., Characterization of chabazite and chabazite like zeolites of unusual composition. *J. Chem. Soc. Faraday Trans.* **1991**, *87*, 1031-1035.

20. Kuznicki, S.M.; Lin, C.C.H.; Bian, J.; Anson, A., Chemical upgrading of sedimentary na-chabazite from bowie, arizona. *Clays Clay Miner.* **2007**, *55*, 235-238.

21. Yazdanbakhsh, F.; Alizadehgiashi, M.; Sawada, J.A.; Kuznicki, S.M., A clinoptilolite-pdms mixed-matrix membrane for high temperature water softening. *Water Sci Technol* **2016**, *73*, 1409-1417.

22. An, W.; Zhou, X.; Liu, X.; Chai, P.W.; Kuznicki, T.; Kuznicki, S.M., Natural zeolite clinoptilolite-phosphate composite membranes for water desalination by pervaporation. *Journal of Membrane Science* **2014**, *470*, 431-438.

23. Adamaref, S.; An, W.; Jarligo, M.O.; Kuznicki, T.; Kuznicki, S.M., Natural clinoptilolite composite membranes on tubular stainless steel supports for water softening. *Water Sci Technol* **2014**, *70*, 1412-1418.

24. Kesraoui-Ouki, S.; Cheeseman, C.; Perry, R., Effects of conditioning and treatment of chabazite and clinoptilolite prior to lead and cadmium removal. *Environmental Science & Technology* **1993**, *27*, 1108-1116.

25. Jang, H.K.; Chung, Y.-D.; Whangbo, S.W.; Lyo, I.W.; Whang, C.N.; Lee, S.J.; Lee, S., Effects of chemical etching with hydrochloric acid on a glass surface. *Journal of Vacuum Science & Technology A: Vacuum, Surfaces, and Films* **2000**, *18*, 2563-2567.

26. Garcia-Basabe, Y.; Rodriguez-Iznaga, I.; de Menorval, L.-C.; Llewellyn, P.; Maurin, G.; Lewis, D.W.; Binions, R.; Autie, M.; Ruiz-Salvador, A.R., Step-wise dealumination of natural clinoptilolite: Structural and physicochemical characterization. *Microporous Mesoporous Mater.* **2010**, *135*, 187-196.

27. Altomare, A.; Corriero, N.; Cuocci, C.; Falcicchio, A.; Moliterni, A.; Rizzi, R., Qualx2.0: A qualitative phase analysis software using the freely available database pow_cod. *J. Appl. Cryst.* **2015**, *48*, 598-603.

28. O'Neill, L., Icdd annual spring meetings. *Powder Diffr.* **2013**, *28*, 137-148.

29. Abuyaghi, A.; El-Bishtawi, R., Removal of lead and nickel ions using zeolite tuff. *J. Chem. Technol. Biotechnol.* **1997**, *69*, 27-34.

30. *Collection of simulated xrd powder patterns for zeolites*. Elsevier: Amsterdam - London - New York - Oxford - Paris - Shannon - Tokyo, 2001; p 586.

31. Keller, E.B.; Meier, W.M.; Kirchner, R.M., Synthesis, structures of alpo4-c and alpo4-d, and their topotactic transformation. *Solid State Ionics* **1990**, *43*, 93-102.

32. Galli, E.; Gottardi, G.; Mayer, H.; Preisinger, A.; Passaglia, E., The structure of potassium-exchanged heulandite at 293, 373 and 593 k. *Acta Crystallogr. Sect. B: Struct. Sci.* **1983**, *39*, 189-197.

33. Koyama, K.; Takeuchi, Y., Clinoptilolite: The distribution of potassium atoms and its role in thermal stability. *Zeitschrift für Kristallographie-Crystalline Materials* **1977**, *145*, 216-239.

34. Levien, L.; Prewitt, C.T.; Weidner, D.J., Structure and elastic properties of quartz at pressure. *Am. Mineral.* **1980**, *65*, 920-930.

35. Arletti, R.; Quartieri, S.; Vezzalini, G., Elastic behavior of zeolite boggsite in silicon oil and aqueous medium: A case of high-pressure-induced over-hydration. *Am. Mineral.* **2010**, *95*, 1247-1256.

36. St. Cloud mining company. <https://www.stcloudmining.com/sales/data-sheets-applications/> accessed 6/4/2021.

37. Oter, O.; Akcay, H., Use of natural clinoptilolite to improve water quality: Sorption and selectivity studies of lead(ii), copper(ii), zinc(ii), and nickel(ii). *Water Environ. Res* **2007**, *79*, 329-335.

38. Inglezakis, V.J.; Loizidou, M.D.; Grigoropoulou, H.P., Equilibrium and kinetic ion exchange studies of pb²⁺, cr³⁺, fe³⁺ and cu²⁺ on natural clinoptilolite. *Water Res.* **2002**, *36*, 2784-2792.

39. Shannon, R., Revised effective ionic radii and systematic studies of interatomic distances in halides and chalcogenides. *Acta Crystallographica Section A* **1976**, *32*, 751-767.

40. Santiago, O.; Walsh, K.; Kele, B.; Gardner, E.; Chapman, J., Novel pre-treatment of zeolite materials for the removal of sodium ions: Potential materials for coal seam gas co-produced wastewater. *SpringerPlus* **2016**, *5*, 571-571.

41. Lippmaa, E.; Samoson, A.; Magi, M., High-resolution aluminum-27 nmr of aluminosilicates. *J. Am. Chem. Soc.* **1986**, *108*, 1730-1735.

42. Holzinger, J.; Nielsen, M.; Beato, P.; Brogaard, R.Y.; Buono, C.; Dyballa, M.; Falsig, H.; Skibsted, J.; Svelle, S., Identification of distinct framework aluminum sites in zeolite zsm-23: A combined computational and experimental 27al nmr study. *The Journal of Physical Chemistry C* **2019**, *123*, 7831-7844.

43. Lippmaa, E.; Maegi, M.; Samoson, A.; Tarmak, M.; Engelhardt, G., Investigation of the structure of zeolites by solid-state high-resolution silicon-29 nmr spectroscopy. *J. Am. Chem. Soc.* **1981**, *103*, 4992-4996.

44. Khodabandeh, S.; Davis, M.E., Synthesis of a heulandite-type zeolite by hydrothermal conversion of zeolite p1. *Chem. Commun.* **1996**, 1205-1206.

45. Malfait, W.J.; Halter, W.E.; Verel, R., 29si nmr spectroscopy of silica glass: T1 relaxation and constraints on the si-o-si bond angle distribution. *Chem. Geol.* **2008**, *256*, 269-277.

46. Minceva, M.; Fajgar, R.; Markovska, L.; Meshko, V., Comparative study of zn²⁺, cd²⁺, and pb²⁺ removal from water solution using natural clinoptilolitic zeolite and commercial granulated activated carbon. Equilibrium of adsorption. *Sep. Sci. Technol.* **2008**, *43*, 1-27.

47. Zendelska, A.; Golomeova, M.; Jakupi, Š.; Lisichkov, K.; Kuvendziev, S.; Marinkovski, M., Characterization and application of clinoptilolite for removal of heavy metal ions from water resources. *Geologica Macedonica* **2018**, *32*, 21-32.

48. Shahack-Gross, R.; Bar-Yosef, O.; Weiner, S., Black-coloured bones in hayonim cave, israel: Differentiating between burning and oxide staining. *Journal of Archaeological Science* **1997**, *24*, 439-446.

49. Akdeniz, Y.; Ülkü, S., Thermal stability of ag-exchanged clinoptilolite rich mineral. *J. Therm. Anal. Calorim.* **2008**, *94*, 703-710.